IEEE Access
Multidisciplinary ⋮ Rapid Review ⋮ Open Access Journal

Received August 18, 2020, accepted August 27, 2020, date of publication September 3, 2020, date of current version September 15, 2020.

Digital Object Identifier 10.1109/ACCESS.2020.3021599

Design of a Limited State Feedback Wide-Area Power System Damping Controller Without Communication Channels

NAGASEKHARA REDDY NAGURU[1], (Member, IEEE), AND YATENDRA BABU GANAPAVARAPU[2], (Member, IEEE)

[1]Stanley College of Engineering and Technology for Women, Hyderabad 500001, India
[2]IIT Hyderabad, Kandi 502285, India

Corresponding author: Nagasekhara Reddy Naguru (ee12p1005@iith.ac.in)

ABSTRACT The wide-area controller (WAC) is used to damp out inter-area oscillations in the power system. Conventionally, to implement WAC in the power system, efficient wide-area communication channels are essential. The performance of the WAC can get degraded with under-performing communication channels. Although, the communication are begin made efficient and redundant, data integrity may pose another threat to the performance of the WAC. In order to subside the dependency on wide-area communication channel, this paper proposes a communication free wide-area controller (CF-WAC) to damp out inter-area oscillations even in the worst scenarios (in terms of communication channels). The CF-WAC is designed based on the state feedback principle and with limited states. The chosen design path can be achieved by using structurally constrained H_2-norm optimization. The proposed CF-WAC is designed in a centralized manner and implemented in a decentralized way and yet retain the near conventional WAC performance. The performance of the proposed CF-WAC is compared with full-scale WAC (FS-WAC i.e., conventional WAC), sparsity-promoting WAC (SP-WAC), and reduced-scale WAC (RS-WAC). Simulation studies are carried out on the IEEE 68-bus test system to evaluate the potential of the CF-WAC in damping inter-area low-frequency oscillations by considering different disturbances and communication channel losses.

INDEX TERMS Centralized design, communication loss, communication free WAC, decentralized design, inter-area oscillations, structurally constrained H_2-norm optimization, wide area control.

I. INTRODUCTION

In an interconnected power system, two kinds of oscillations can happen frequently termed as local and inter-area mode oscillations [1]. The local mode oscillations can be damped out effectively by designing the power system stabilizers (PSSs) based upon local signals [2]. On the other hand, since PSSs use local input signals, these are not sufficient to damp out inter-area oscillations. Therefore, the wide-area controller (WAC) is required to overcome the shortfalls of local damping controllers [3], [4]. However, in reality, the WAC requires information from remote locations. With the advancements in wide-area monitoring systems (WAMS) [5], like phasor measurement units (PMUs), it is possible to transfer the synchronized measurements of the entire power system to the control center in short-span of time. After receiving the data at the control center, the WAC will utilize the system-wide information and delivers the corrective signal to damp out inter-area oscillations. The WAC can be designed by using either state feedback [6] or an output feedback control technique [3]. In a state feedback control technique, an additional state estimator is required to estimate the system states. The estimated system states are used in later stages along with a state feedback gain matrix to generate control signals at the control center to damp out oscillations. On the other hand, the output feedback control technique does not require a state estimator. Therefore, in the output feedback controller, the control signals are generated directly by passing the data received from WAMS to a WAC gain matrix (i.e., feedback gain matrix). In general, for both the cases, the WAC gain matrix is deployed at a centralized control center. The state feedback gain matrix

The associate editor coordinating the review of this manuscript and approving it for publication was Ying Xu.

can be developed by using either classical LQR control technique [7] or H_2-norm optimization technique without adding constraints [8]. In [9], a sparsity promoting WAC (SP-WAC) is proposed to design the state feedback gain matrix that promotes sparsity in the feedback gain matrix. In [10], a reduced scale WAC (RS-WAC) design is intended by using dominance index analysis. Similarly, the output feedback gain matrix can be designed by using H_∞ control technique or mixed H_∞/H_2 control techniques [11]. Several other approaches are proposed in the literature [12]–[15] to design the feedback gain matrix that is used at the control center.

The main issues in designing the wide-area control system are the necessity of reliable communication channels, availability of continuous PMU measurements, time delay, and so on. The performance of the WAC can be deteriorated because of either communication loss or delay in PMU signals. To overcome the time delay issues, few methodologies are proposed in the literature [16], [17]. In [17], a Kalman filtering methodology is proposed to compensate the time delay effects. However, in some situations, it may be difficult to compensate for the time delays because of large communication paths that are established between the wide-area control center and the system components. On the other hand, the lag or loss in PMU reporting can deteriorate the performance of the wide-area controller. Moreover, depending upon the system size, the commissioning cost can be increased if the WAC requires more remote signals. Another severe problem in a wide-area control system is the loss of communication signals. Therefore, to overcome these communication loss issues, it is necessary to design a WAC that must exhibit robust performance under different scenarios. In [18], a systematic procedure to develop a fault-tolerant WAC is illustrated in detail. A wide-area damping controller is proposed in [15] furnishing good damping performance under communication failures. In [19], a fault-tolerant WAC is proposed to damp out inter-area oscillations under different disturbances. In [20], a GrHDP based WAC is developed to tolerate various communication failures. In all these fault-tolerant wide-area control systems, minimum communication channels are mandatory to provide proper damping performance at the controller output side. Therefore, to overcome these issues, this article proposes a communication free wide-area controller to damp out inter-area oscillations without using any remote signals.

The primary contribution of this paper is to develop a wide-area controller which requires no communication paths. Here, the wide area controller is implemented by using state feedback control technique. In a state feedback control technique, the inputs to the wide area controller are system states. However, the most participating states in inter-area mode oscillations are generator speed and angle [2]. Therefore, it is enough to design a controller with speed and angle inputs alone to damp out inter-area mode oscillations. The required state feedback gain matrix is designed by employing structurally constrained H_2-norm optimization technique. The design of gain matrix can be done in a centralized level. After calculating the gain matrix, take out the respective columns and rows of gain matrix related to each and every generator's speed and angle states. Now, the controller output signals to the generator excitation system can be calculated by taking the product of speed and angle states and gain matrix of that generator. The required speed and angle states of generator can be estimated by using speed and position estimation algorithm which are available in literature [21]. In this paper, it is assumed that the speed and angle states of generator are readily available.

The rest of the article is organized as follows. In Section II, the outline of the proposed methodology is presented. The mathematical formulation of the proposed methodology is provided in Section III. In Section IV, the design and analysis of all controllers are verified by considering 68-bus test system. The comparative performance analysis between all controllers are analyzed by considering time delay in the communication channels in Section V. In Section VI, the comparative performance is analyzed considering communication failure on the controller input and output sides. The discussion between all controllers are presented in Section VII. Finally, the article is concluded in Section VIII.

II. OUTLINE OF THE PROPOSED WIDE-AREA CONTROLLER (CF-WAC) DESIGN

A. OUTLINE OF FS-WAC, SP-WAC, AND RS-WAC

Fig. 1(a.) represents the general WAC architecture layout of FS-WAC, SP-WAC, and RS-WAC. All these controllers are implemented with the help of the state feedback control technique. The main function of a PMU is to transfer the voltage and current signals to the control center through the WAM network. The global positioning system (GPS) is used to provide time stampings to the PMU data. After receiving the signals at the control center, the required dynamic states are estimated by using a state estimator, which is shown in Fig. 1(a.). The state estimator can be implemented by using either an extended Kalman filter (EKF) [22] or an unscented Kalman filter (UKF) [23]. Then, the WAC system's output signals can be calculated by taking the product of system states and feedback gain matrix. These WAC output signals are transmitted to the generators' excitation system with the help of a WAC communication network.

As mentioned earlier, the generated WAC signals are given to the generators' excitation system, as shown in Fig. 1(b.). Acronym AVR represents the automatic voltage regulator, and ESS represents the excitation system stabilizer. From Fig. 1(a.), it can be observed that the feedback gain matrix and required dynamic states are varied from one control to another control. In FS-WAC, at the input side, all generator states are estimated, and the required feedback gain matrix can be calculated by using the classical state feedback control technique. In SP-WAC, the required input states are not predefined, and the output signals are also not predefined. Thus, the structure of feedback gain matrix and system states

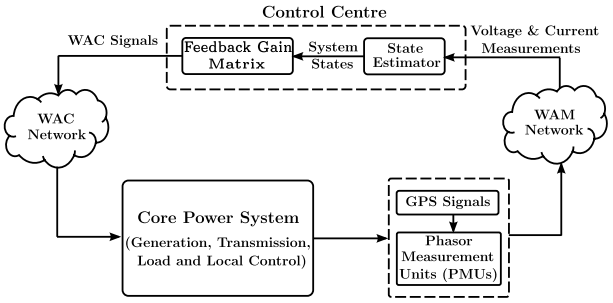

(a.) Overall layout.

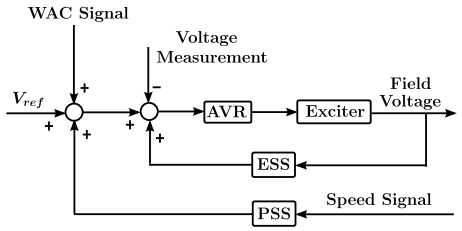

(b.) Excitation control system.

FIGURE 1. The state feedback control based WAC system architecture.

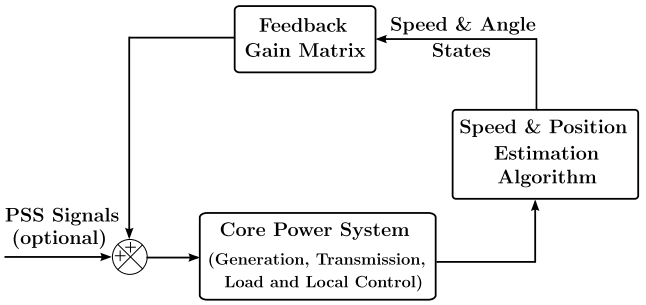

FIGURE 2. The proposed CF-WAC system architecture.

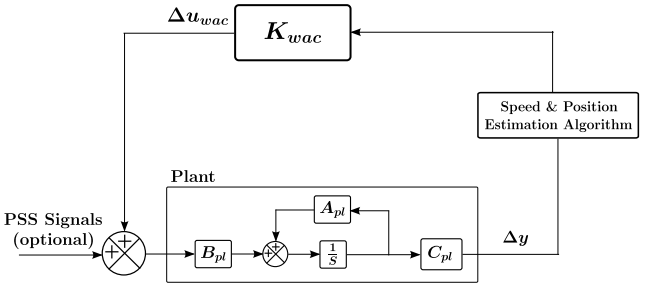

FIGURE 3. The schematic layout of the proposed CF-WAC system.

are formed by promoting sparsity [9]. Finally, in RS-WAC, the input signals are dominant generator states alone, and the output signals are given to the same dominant generators. For all these control techniques, the WAM network becomes highly constrained because it requires measurements from many generators. Therefore, it leads to costly WAM infrastructure.

B. OUTLINE OF THE PROPOSED CF-WAC

The proposed WAC architecture layout with feedback gain matrix is represented in Fig. 2. As mentioned earlier, the most dominating states in inter-area mode oscillations are rotor speed and angle. Therefore, it is good enough to obtain the speed and angle states in real-time for damping out inter-area oscillations. The primary function of a speed & position estimation algorithm is to estimate the speed and angle states in real-time. These states can be estimated locally and multiplied with the respective feedback gain matrix structure to obtain the WAC signals. In centralized manner, the structurally constrained H_2-norm optimization technique can be used to design the state feedback gain matrix. Initially, the feedback gain matrix is full matrix. It means that the feedback gain matrix having centralized structure and those values are related to all system states. Later, it can be designed to decentralized structures corresponding to all generators speed and angle states alone by maintaining the system stability.

In this paper, the decentralized generated WAC signals along with the PSS signals (optional) are fed to the excitation system of generators and it is shown in Fig. 3. It is to be noted that the objective of this particular work is to design the communication free wide area controller, not the power system stabilizer. The PSSs should be locally tuned beforehand by using any of the available techniques. After designing the PSSs, those should be included in the core power system model for the further investigation of inter-area oscillations. However, in this article, the PSSs signals are not included to the generator's excitation system to validate the effectiveness of the WAC alone.

III. MATHEMATICAL FORMULATION OF THE PROPOSED CF-WAC

In this section, the mathematical formulation of proposed CF-WAC, FS-WAC, SP-WAC, and RS-WAC is illustrated. Consider the linearized state-space model of the total system, as shown in Fig. 3 is described as follows:

$$\Delta\dot{\boldsymbol{x}} = \boldsymbol{A}\Delta\boldsymbol{x} + \boldsymbol{B_u}\Delta\boldsymbol{u_{wac}} + \boldsymbol{B_w}\Delta\boldsymbol{w} \tag{1}$$

$$\Delta\boldsymbol{y} = \boldsymbol{C_y}\Delta\boldsymbol{x} \tag{2}$$

$$\Delta\boldsymbol{z} = \boldsymbol{C_z}\Delta\boldsymbol{x} + \boldsymbol{D_z}\Delta\boldsymbol{u_{wac}}. \tag{3}$$

where x is the state vector, u_{wac} is the wide area control signal, w is the disturbance input vector, z is the performance output vector, and y is the measurement vector. Parameters $\boldsymbol{B_w}$, $\boldsymbol{C_z}$ and $\boldsymbol{D_z}$ are to be specified by the user depending upon the specific performance requirement. Typically, $\boldsymbol{C_z}$ and $\boldsymbol{D_z}$ are chosen as follows.

$$\boldsymbol{C_z}^T = \begin{bmatrix} \boldsymbol{Q}^{\frac{1}{2}} & \boldsymbol{0} \end{bmatrix} \tag{4}$$

$$\boldsymbol{D_z}^T = \begin{bmatrix} \boldsymbol{0} & \boldsymbol{R}^{\frac{1}{2}} \end{bmatrix}. \tag{5}$$

That is, $\boldsymbol{z}$ is chosen as an $(N_s + N_s) \times 1$ vector to represent both the control effort as well as the state disturbance. Here, N_s gives the number of state variables in the system. Matrices

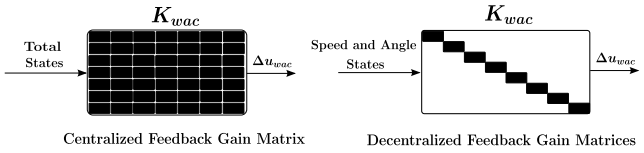

FIGURE 4. The structure of the proposed CF-WAC feedback gain matrix.

$\boldsymbol{Q}$ and $\boldsymbol{R}$ are similar to those in the LQR control. Both are symmetric matrices. Matrix $\boldsymbol{Q}$ should be positive semidefinite, whereas, matrix $\boldsymbol{R}$ should be positive definite. The selection of $\boldsymbol{B_w}$ depends upon the specific set of physical disturbances that are recognized as prime threats to the system. There is a scope of research for appropriately determining the value of $\boldsymbol{B_w}$ for a power system. The WAC signals that are used for the excitation system are generated by using the following equation.

$$\boldsymbol{\Delta u_{wac}} = \boldsymbol{K_{wac}}\,\boldsymbol{\Delta x}. \tag{6}$$

A. CF-WAC FORMULATION

For the proposed CF-WAC, the number of rows in $\boldsymbol{K_{wac}}$ is equal to the number of generators. All columns of the $\boldsymbol{K_{wac}}$ matrix except generators' speed and angle states columns should be set to zeros. The same is illustrated in Fig. 4. This, in turn, eliminates the need for establishing communication paths between remote locations and wide area control centre. In addition, certain states are usually not observable. The corresponding columns of the $\boldsymbol{K_{wac}}$ matrix should also be set to zeros. Finally, the $\boldsymbol{K_{wac}}$ structure consists of only generators' speed and angle states. Therefore, only generators' speed and angle states are considered to generate the required WAC signals.

In this paper, the proposed CF-WAC is designed by means of the H_2-norm optimization with structural constraints. As it is known that, the H_2-norm optimized controller exhibits superior transient performance compared to the H_∞-norm optimized controller. Moreover, forcing some columns to become zeros imposes structural constraints on $\boldsymbol{K_{wac}}$. Thus, it would be difficult to obtain the H_∞-norm optimized solution of the state feedback controller. For the dynamic system model (1), (2), (3), (4) and (5), the H_2-norm optimization can be formulated as follows.

$$\text{Minimize} \quad \left\{\text{trace}\left(\boldsymbol{B_w}^T \boldsymbol{F} \boldsymbol{B_w}\right)\right\} \tag{7}$$

$$s.t.\ \boldsymbol{F}\left(\boldsymbol{A}+\boldsymbol{B_u}\boldsymbol{K_{wac}}\right)+\left(\boldsymbol{A}+\boldsymbol{B_u}\boldsymbol{K_{wac}}\right)^T\boldsymbol{F} + \left(\boldsymbol{C_z}+\boldsymbol{D_z}\boldsymbol{K_{wac}}\right)^T\left(\boldsymbol{C_z}+\boldsymbol{D_z}\boldsymbol{K_{wac}}\right)=\boldsymbol{0} \tag{8}$$

$$\boldsymbol{K_{wac}} \circ \boldsymbol{\Theta} = \boldsymbol{0} \tag{9}$$

$$\left(\boldsymbol{A}+\boldsymbol{B_u}\boldsymbol{K_{wac}}\right) \prec \boldsymbol{0}. \tag{10}$$

More details about the H_2-norm optimization with and without structural constraints objective function can be found in [24]. To obtain the required CF-WAC feedback gain matrix, heavy penalties are assigned to the elements that are set to be zero, and no penalty can be added for the elements that are to be left free. The step by step procedure to design CF-WAC is as follows.

Step 1 – Perform small-signal stability analysis to find out eigenvalues of the system.
Step 2 – Identify the inter-area modes of the system.
Step 3 – Find out the full scale K_{wac} matrix assuming that all generator states are available.
Step 4 – Define the structure of required CF-WAC matrix according to speed & angle states of all generators.
Step 5 – Apply the structural H_2-norm optimization to get the CF-WAC matrix.
Step 6 – Now, separate the CF-WAC matrix in a decentralized manner to send the WAC signals in a decentralized manner.

B. FS-WAC FORMULATION

In FS-WAC formulation, the controller inputs are all generators' states, and output signals are given to all generators' excitation systems. Therefore, it is a full matrix, and it is calculated by using the classical Linear Quadratic Regulator (LQR) technique. The same can be achieved by solving a H_2-norm optimization technique without adding constraints, as shown in equation (7).

C. SP-WAC FORMULATION

In SP-WAC formulation, the controller inputs and outputs are defined by creating sparsity [9] in the feedback gain matrix ($\boldsymbol{K_{wac}}$). The sparsity is defined as follows:

$$\boldsymbol{\Theta}_{ij} = 1/|\boldsymbol{K_{wac}}_{ij}|, \quad \boldsymbol{K_{wac}}_{ij} \neq 0;$$
$$\boldsymbol{\Theta}_{ij} = 1/\epsilon, \quad \boldsymbol{K_{wac}}_{ij} = 0,\ 0 < \epsilon < 1.$$

where $\boldsymbol{\Theta}_{ij}$ values chosen to be inversely proportional to the magnitude of $\boldsymbol{K_{wac}}_{ij}$ to define the sparsity in the feedback gain matrix ($\boldsymbol{K_{wac}}$). More details about SP-WAC can be found in [9].

D. RS-WAC FORMULATION

The selection of inputs and outputs in RS-WAC design are calculated by performing dominance index analysis [10]. Total generators are classified into dominant and non-dominant generators by using dominance index analysis. Dominant generators refers to the generators with highest participation in inter-area oscillation modes. Therefore, the inputs in RS-WAC formulation are dominant generator states alone. The outputs of RS-WAC are given to the dominant generators only. The steps involved in RS-WAC design are as follows:

Step 1 – Perform small-signal stability analysis to find out eigenvalues of the system.

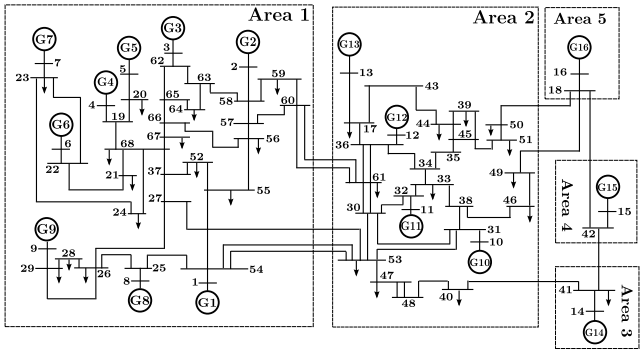

FIGURE 5. The 68-bus test system.

TABLE 1. Inter-area oscillation modes.

Mode Index	Eigenvalues	Damping ratio (ζ)	Frequency (f) in Hz
1	$-0.0508 \pm 2.453i$	0.0207	0.3905
2	$-0.0871 \pm 3.278i$	0.0266	0.5217
3	$-0.0724 \pm 3.758i$	0.0193	0.5981
4	$-0.2394 \pm 4.982i$	0.0480	0.7931

Step 2 – Identify the inter-area modes of the system.

Step 3 – Find out the participation factors of states that are involved in inter-area mode oscillations.

Step 4 – Find out each generator's dominance index.

Step 5 – Identify the dominant and non-dominant generators of the system.

More details about RS-WAC can be found in [10].

IV. DESIGN AND ANALYSIS OF FS-WAC, SP-WAC, RS-WAC, AND CF-WAC FOR THE 68-BUS TEST SYSTEM

The effectiveness of the proposed fault-tolerant wide-area controller is validated by considering the 68-bus test system, which is shown in Fig. 5. Moreover, the proposed controller's performance is compared with different wide area controllers, which are mentioned in the previous section. The test system consists of 16 generators, and each generator is provided with IEEE-ST1A type exciters. Exciter limits are set between 5 and -5 p.u. The modeling of generators is represented with sub-transient type, and loads are modeled by using a constant impedance model. The mechanical input torque of every generator is assumed to be constant. More information about the test system can be found in [1].

Table 1 gives the information about inter-area oscillation modes of the particular test system in the absence of wide area controller. It has 4 inter-area modes. Columns 3 and 4 of Table 1 gives the information about each mode damping ratio and frequency.

A. DESIGN OF FS-WAC, SP-WAC, RS-WAC, AND CF-WAC

As mentioned earlier, the WAC can be implemented by using either state feedback or output feedback control technique.

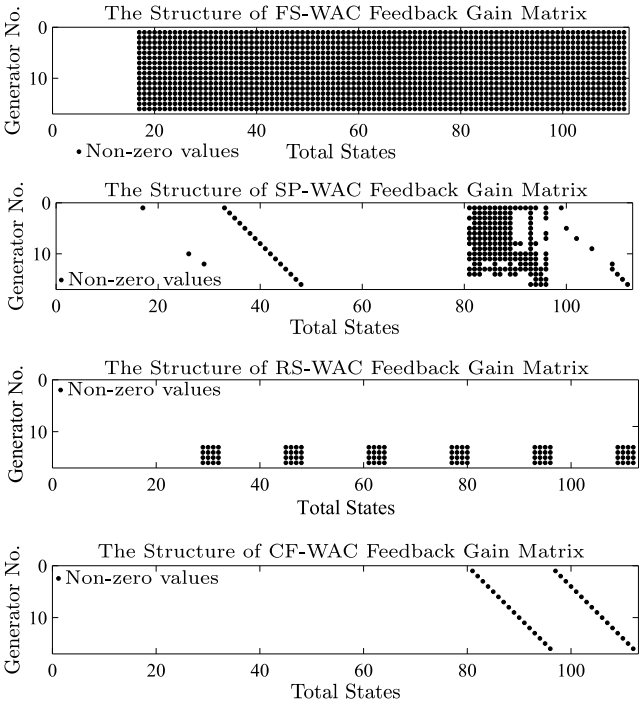

FIGURE 6. The structure of FS-WAC, SP-WAC, RS-WAC, and CF-WAC feedback gain matrices.

In this article, the WAC is implemented with state feedback control technique. FS-WAC uses all generator states as inputs to generate the WAC output signals. In other words, FS-WAC (full scale WAC) is the basic WAC using state feedback approach. Therefore, the WAC and FS-WAC both are same in this case. FS-WAC, SP-WAC, RS-WAC, and CF-WAC design for the test system shown in Fig. 5 is explained in this subsection. The structures of FS-WAC, SP-WAC, RS-WAC, and CF-WAC feedback gain matrices are shown in Fig. 6. Rows represents the number of generators and columns represents the total system states. In these matrices structures, dots represents the non-zero values and empty space represents zeros. FS-WAC uses all system states on the input side and transmitting signals to all generators on the output side. The feedback gain matrix ($\boldsymbol{K_{wac}}$) of FS-WAC is designed by using the classical LQR control technique. This is achieved by solving the equation (7) without imposing constraints. In the classical LQR control technique, the matrix $\boldsymbol{R}$ taken as identity matrix and matrix $\boldsymbol{Q}$ set as a diagonal matrix. The diagonal entry corresponding to an angle or speed state is set to 100. All other diagonal entries are set to 0. The feedback gain matrix ($\boldsymbol{K_{wac}}$) can be modified for SP-WAC, RS-WAC, and CF-WAC based upon the design. The design of SP-WAC is illustrated in [9]. In this case, the structure of the feedback gain matrix depends upon the weights of the matrix. RS-WAC is designed by using dominant generators alone. RS-WAC uses dominant generators' states on the input side and transmitting the signals to the same dominant generators' excitation systems. The dominant generators for the test system are calculated by applying the dominance index analysis. The dominant

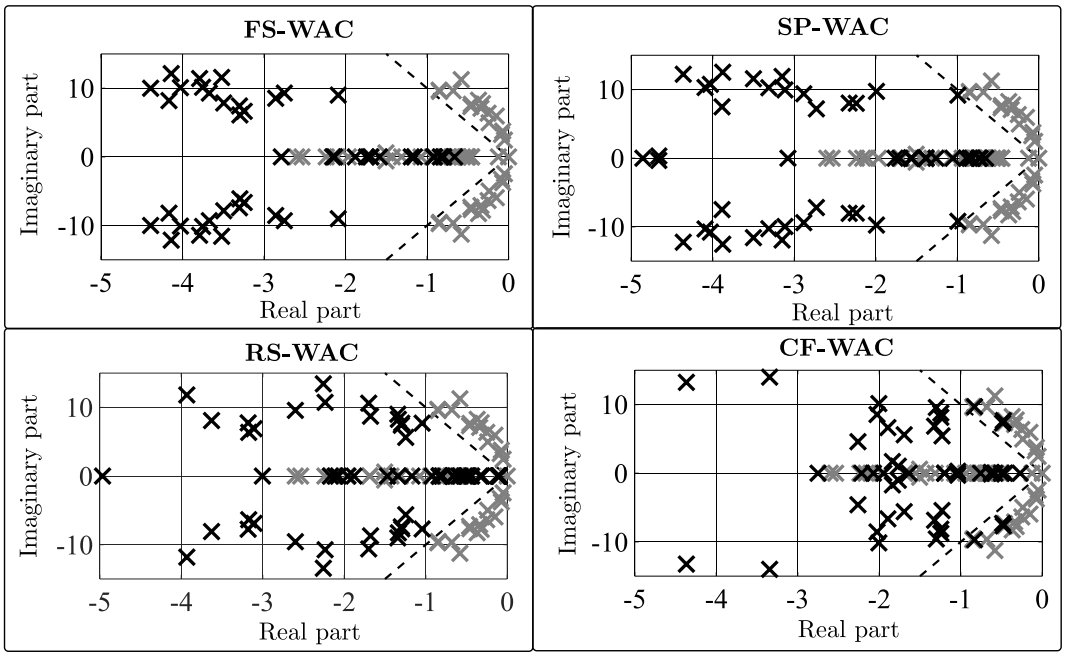

FIGURE 7. Eigenvalues of the test system with out and with WACs.

generators are G13, G14, G15, and G16. CF-WAC is designed by using speed and angle states of all generators on the input side and providing signals to all generators on the output side. The design of the CF-WAC is completely offline procedure. The design task may be repeated if the corresponding system subjected to a significant architectural changes. On the other hand, the run-time efficiency is indeed very critical to the success of any WAC. In a centralized regime, as the scale of the system increases, the controller processing burden also increases, which surfaces the scalability issues in the implementation. However, the proposed approach is devised to be a decentralized run-time process, i.e., the CF-WAC is distributed over the system. Each decentralized module takes only the corresponding local measurements. Hence, the processing burden is also distributed over the network. Therefore, the scalability concerns are eliminated through decentralized implementation.

B. TIME AND FREQUENCY DOMAIN ANALYSIS

The eigenvalues of the test system are calculated by performing small signal stability analysis. The eigenvalues of the test system with FS-WAC, SP-WAC, RS-WAC, CF-WAC and with out WAC for normal operating point are shown in Fig. 7. It can be seen that some of the eigenvalues are lying behind the 10% damping line in the absence of wide area controller. On the other hand, with FS-WAC, SP-WAC, RS-WAC and CF-WAC, the eigenvalues of test system are moved towards the left. Non-linear simulation studies are carried out to validate the effectiveness of the proposed controller performance. The time domain analysis is accomplished by considering different disturbances that are represented in Table 2.

TABLE 2. List of disturbances considered.

Disturbance id	Type of disturbance	Location	Time
TL_OUT	Line outage	Between Buses 60 and 61	At 2.5 sec
LD_SHD	Load shedding	At Bus 23	At 2.5 sec
3_PH_FLT	Three phase fault	At Bus 59	At 2.5 sec

TABLE 3. The settling times of all generators considering line outage between buses 60 and 61.

Gen. Id	FS-WAC	SP-WAC	RS-WAC	CF-WAC
G1	4.2008	6.1171	11.2729	15.2871
G2	3.3365	4.7687	12.0364	18.4921
G3	3.2093	4.9703	12.0038	21.0448
G4	4.0374	5.0602	13.0901	22.0763
G5	4.1555	4.4937	14.6107	23.4381
G6	4.0938	5.0467	13.0900	23.1987
G7	4.0839	6.5280	12.6508	22.1127
G8	4.0404	4.9746	11.2838	21.5982
G9	4.7564	9.0506	15.0283	16.5432
G10	4.0776	6.2364	9.5887	15.5062
G11	3.6880	5.6243	9.7000	20.1000
G12	3.7359	6.4645	9.1190	21.8193
G13	4.0198	5.8622	9.1487	12.5077
G14	4.5357	5.8589	11.8543	17.6271
G15	4.3266	5.3907	7.9544	19.5275
G16	5.1210	5.4181	12.3135	17.1647

1) LINE OUTAGE BETWEEN BUSES 60 AND 61

In this subsection, the controller performances are evaluated by disconnecting the one of the line between buses 60 and 61. The corresponding dynamic responses of rotor angle of generator 13 (G13), terminal active power of generator 13 (G13) and active power flow in line connected

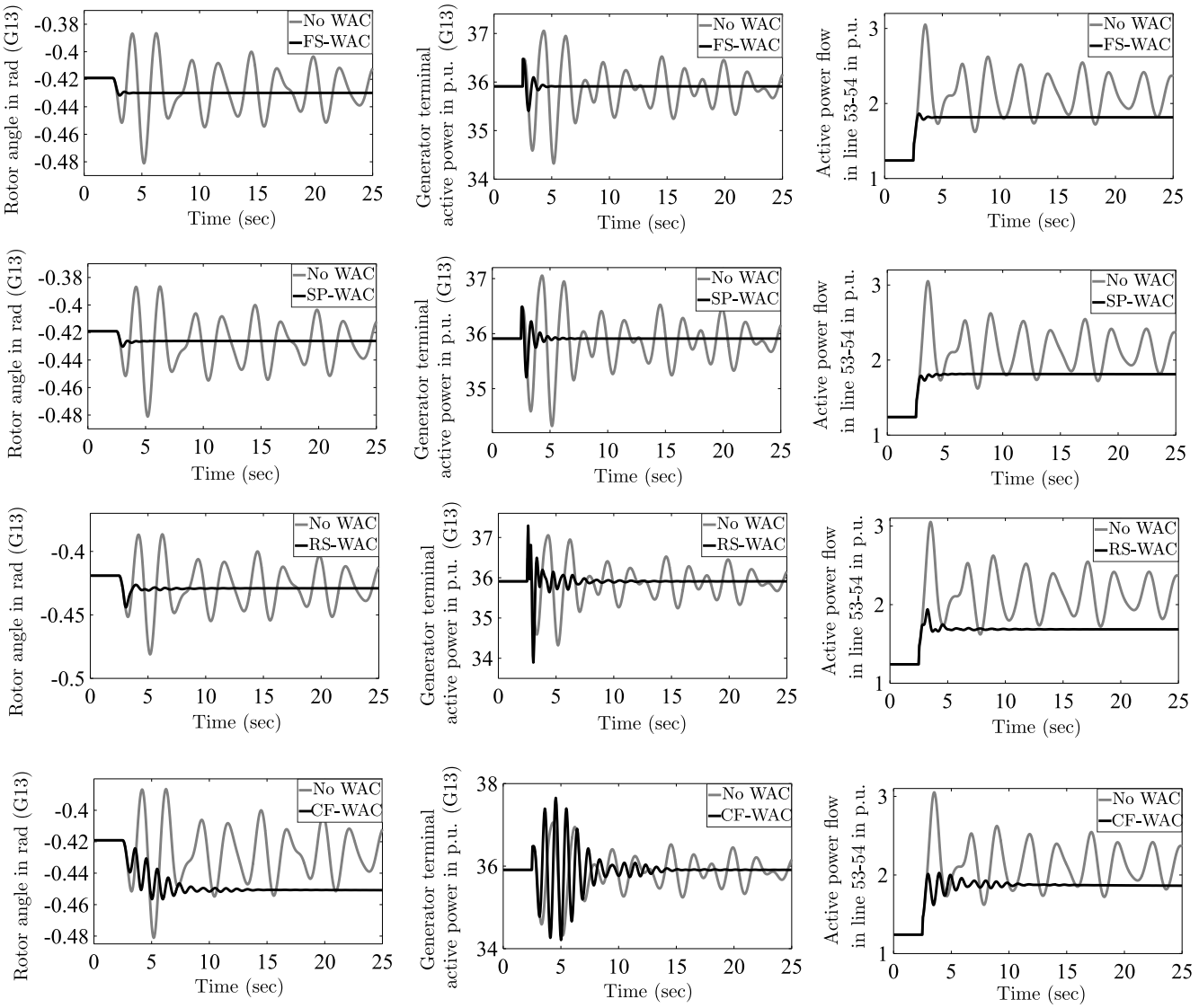

FIGURE 8. The dynamic simulation waveforms for the line outage between buses 60 and 61 with and without WAC.

between buses 53 and 54 are shown in Fig. 8. It can be seen that the oscillations which are occurred in the absence of controller are damped out by employing different controllers (FS-WAC, SP-WAC, RS-WAC and CF-WAC). The comparison between these controllers are shown in Table 3 in the form of settling times. The settling times are calculated by considering 2% tolerance band. It can be observed that FS-WAC gives the good performance compared to the remaining controllers. However, as mentioned earlier, FS-WAC needs the information from all PMUs. Likewise, SP-WAC and RS-WAC also requires the information from some PMUs. Whereas, CF-WAC doesn't requires any information from PMUs.

2) LOAD SHEDDING AT BUS 23

By considering load shedding at bus 23, the performance of FS-WAC, SP-WAC, RS-WAC, and CF-WAC are shown in Fig. 9. It can be observed that the oscillations are effectively damped out with the incorporation of wide-area controllers. The corresponding settling times are listed in Table 4. The settling times of all generators are close to 10 sec when FS-WAC and SP-WAC are employed.

3) THREE PHASE FAULT AT BUS 59

The effectiveness of controllers are evaluated by applying three phase fault at bus 59. The fault is immediately cleared by opening the lines which are connected to that particular bus. The dynamic responses are shown in Fig. 10. In addition, the corresponding settling times of all generators are shown in Table 5. It is observed that the settling times of all generators are close to 20 sec when RS-WAC and CF-WAC are employed.

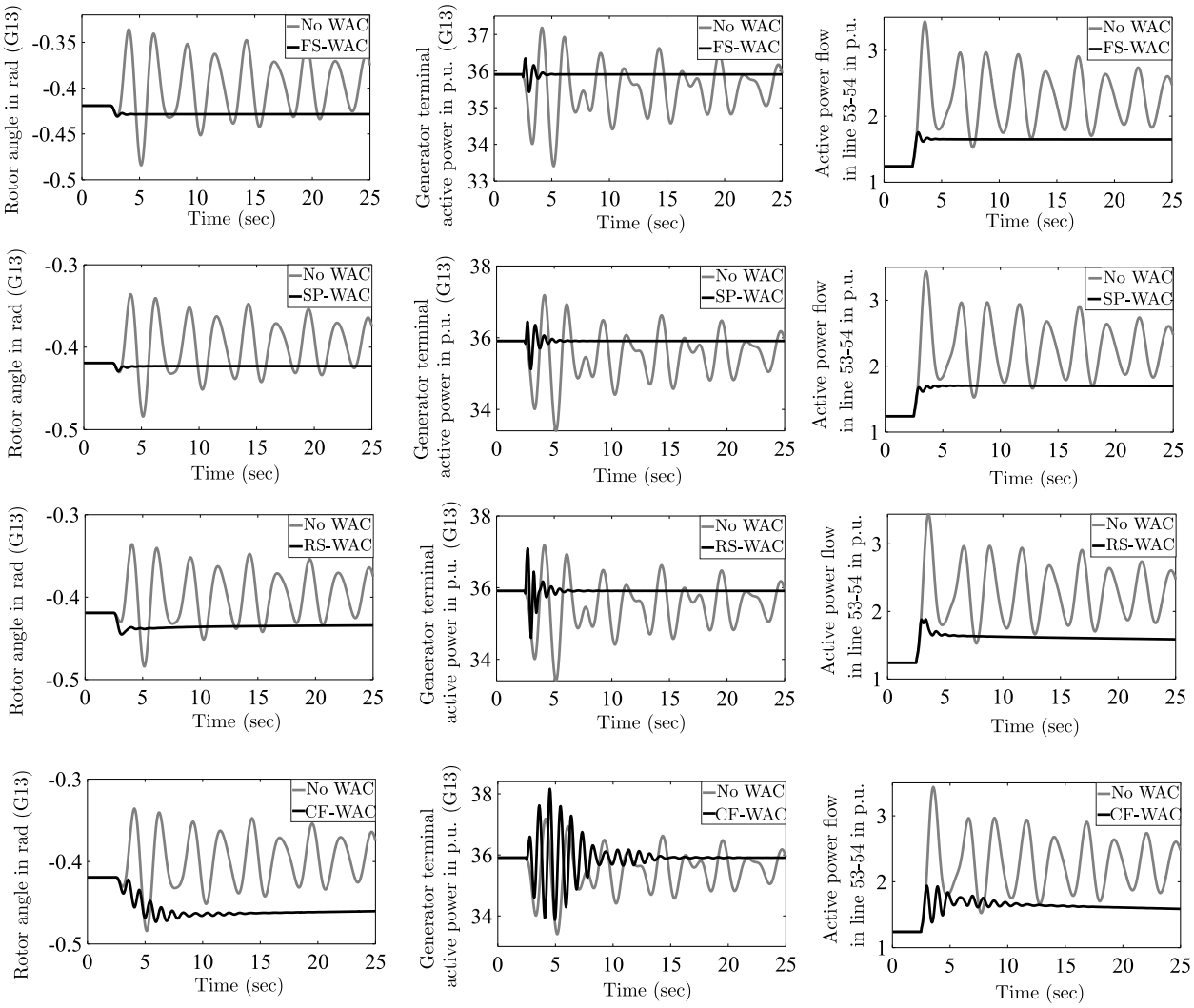

FIGURE 9. The dynamic simulation waveforms for the load shedding at bus 23 with and without WAC.

TABLE 4. The settling times of all generators considering load shedding at bus 23.

Gen. Id	FS-WAC	SP-WAC	RS-WAC	CF-WAC
G1	4.4732	7.0839	21.5939	22.6567
G2	5.4815	5.0999	10.7631	22.6787
G3	4.8762	5.1203	21.5740	19.5846
G4	4.0665	4.7790	21.7872	23.5891
G5	5.6149	4.3590	21.9794	22.6589
G6	3.3666	4.4669	21.6926	23.2071
G7	3.0676	3.6338	22.6208	20.0018
G8	4.7587	4.9654	21.5454	23.9782
G9	5.4904	7.5703	7.9050	19.7081
G10	6.2176	6.2661	5.6354	20.9905
G11	4.7929	5.6974	15.3307	23.0737
G12	5.5116	7.4298	20.6086	21.0700
G13	4.0754	5.9325	21.2323	21.2659
G14	4.5518	4.8256	18.5233	22.2071
G15	4.1988	4.7969	20.9228	23.0376
G16	3.6353	4.7733	14.3759	14.4941

TABLE 5. The settling times of all generators considering three phase fault at bus 59.

Gen. Id	FS-WAC	SP-WAC	RS-WAC	CF-WAC
G1	4.2173	12.0060	20.6022	21.6293
G2	3.1337	4.2229	11.8947	18.1929
G3	3.2196	4.3511	20.4095	21.5222
G4	4.8133	10.9841	22.7470	21.6337
G5	11.1095	15.9712	22.0599	22.9321
G6	4.8470	10.0002	22.3246	23.1310
G7	4.8510	14.1596	22.4057	23.5986
G8	4.2528	9.2049	20.9648	21.9883
G9	10.5289	19.3599	6.9077	13.3103
G10	5.4837	5.6274	7.7938	16.1771
G11	4.7939	5.0042	19.8427	15.6846
G12	6.7985	6.7487	21.0818	21.6340
G13	4.0345	5.8145	20.6128	13.3886
G14	5.1851	6.8974	20.1354	12.4449
G15	4.1789	4.5727	11.2336	21.2758
G16	3.6261	6.9464	17.4357	19.2585

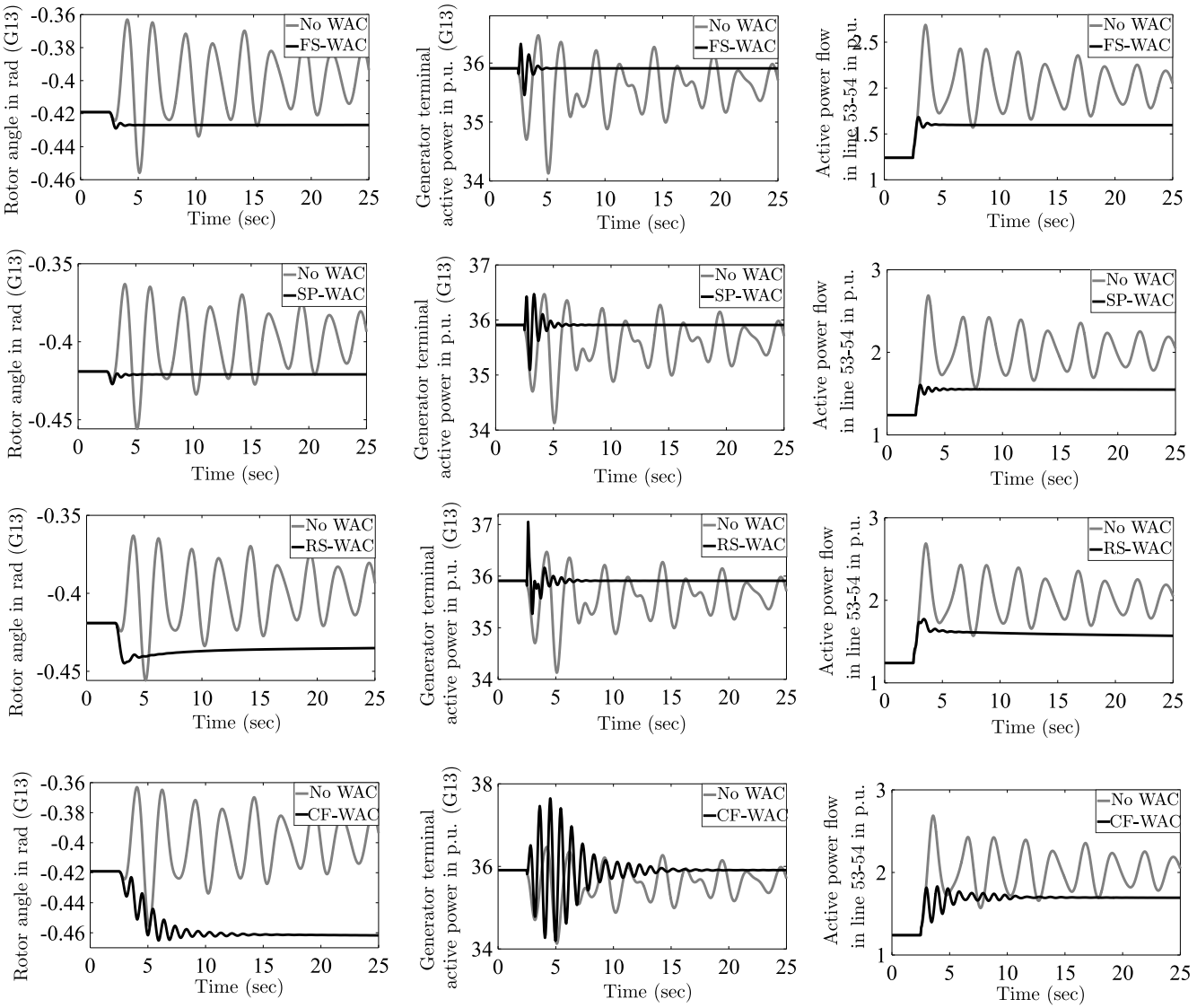

FIGURE 10. The dynamic simulation waveforms for the three phase fault at bus 59 with and without WAC.

V. COMPARATIVE PERFORMANCE EVALUATION CONSIDERING DELAY IN THE COMMUNICATION NETWORK

In order to verify the potential of the different wide-area damping controllers, it is assumed that the transmission delay in the communication channels is fixed on the input and output sides of the controller. The fixed time delay of 200 ms considered on input and output sides. Therefore, the total time delay in the WAC loop is 400 ms. Traditional Pade approximation [6] is used to model the time delay in this paper. The transfer function of this time delay is included in the original plant model (equations (1)-(3)) for the analysis. The line outage between buses 60 and 61 along is considered for the time-domain simulation. As mentioned earlier, the fixed time delay of 200 ms is included in the input and output sides. Fig. 8 represents the dynamic simulation waveforms of different wide-area damping controllers. The proposed CF-WAC does not require any communication paths. Hence, it is free from time delay issues. From the plots shown in Fig. 8, it can be observed that the SP-WAC gives the good damping performance compared to the remaining controllers. On the other hand, the proposed CF-WAC gives satisfactory performance compared to the remaining controllers (FS-WAC and RS-WAC).

VI. COMPARATIVE PERFORMANCE EVALUATION CONSIDERING COMMUNICATION FAILURE

The performance of the wide-area controller mainly depends upon input signals which are acquired from PMUs and output signals, which are transmitted to the power system. Therefore, in this subsection, the effectiveness of controllers are validated by considering communication loss on input and output sides. Line outage between buses 60 and 61 is considered.

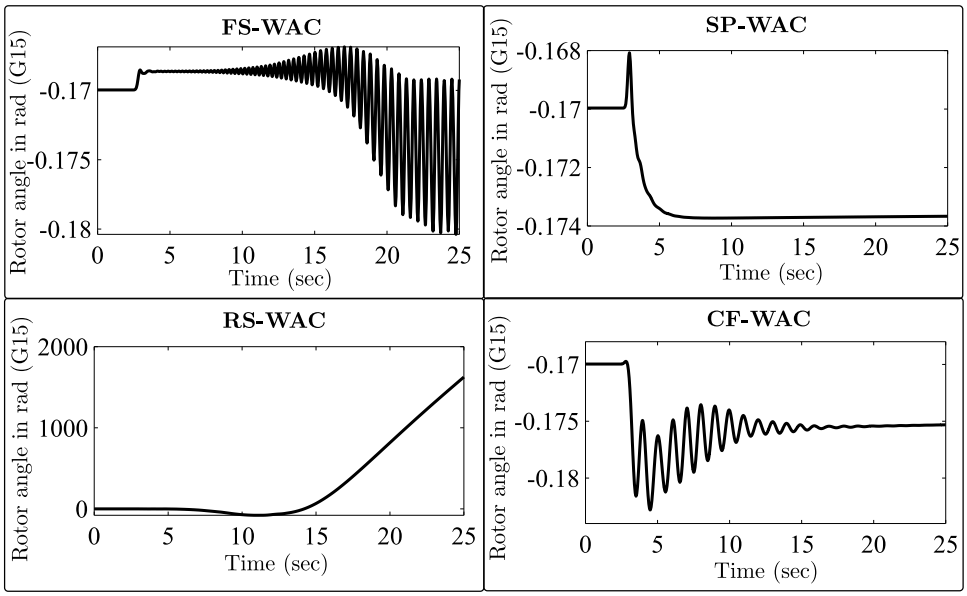

FIGURE 11. The rotor dynamic waveforms of generator 15 (G15) considering the fixed time delay of 200 ms.

TABLE 6. The settling times of all generators considering one communication failure on output side.

Gen. Id	FS-WAC	SP-WAC	RS-WAC	CF-WAC
G1	4.2655	8.0726	Unstable	15.2871
G2	3.1296	4.8980	Unstable	18.4921
G3	3.2146	5.0097	Unstable	21.0448
G4	5.4980	5.0728	Unstable	22.0763
G5	7.2750	4.9323	Unstable	23.4381
G6	5.4965	5.0597	Unstable	23.1987
G7	5.5340	7.5579	Unstable	22.1127
G8	5.4686	4.9916	Unstable	21.5982
G9	7.2651	9.5971	Unstable	16.5432
G10	5.5009	6.3930	Unstable	15.5062
G11	5.4682	6.3550	Unstable	20.1000
G12	5.4269	8.3680	Unstable	21.8193
G13	6.2751	6.6598	Unstable	12.5077
G14	9.6633	5.4328	Unstable	17.6271
G15	15.5528	9.0715	Unstable	19.5275
G16	20.1559	5.5450	Unstable	17.1647

TABLE 7. The settling times of all generators considering two communication failures on controller output side.

Gen. Id	FS-WAC	SP-WAC	RS-WAC	CF-WAC
G1	13.4563	9.4721	Unstable	15.2871
G2	11.5237	4.8753	Unstable	18.4921
G3	12.4169	5.4062	Unstable	21.0448
G4	15.9846	7.3364	Unstable	22.0763
G5	16.0988	10.5606	Unstable	23.4381
G6	15.9573	7.3166	Unstable	23.1987
G7	15.9995	10.6158	Unstable	22.1127
G8	16.0263	7.2513	Unstable	21.5982
G9	17.6348	12.2982	Unstable	16.5432
G10	16.9121	13.2628	Unstable	15.5062
G11	17.6818	11.5805	Unstable	20.1000
G12	16.9816	12.1148	Unstable	21.8193
G13	16.6428	16.4449	Unstable	12.5077
G14	18.5764	14.9585	Unstable	17.6271
G15	23.0805	18.1906	Unstable	19.5275
G16	20.2410	14.9316	Unstable	17.1647

A. LOSS OF ONE COMMUNICATION SIGNAL ON CONTROLLER OUTPUT SIDE

Here, the performances of FS-WAC, SP-WAC, RS-WAC, and CF-WAC are evaluated by considering communication loss of transmitted signal to the generator 15 (G15). Fig. 12 represents the waveforms with the incorporation of individual controllers: FS-WAC, SP-WAC, RS-WAC, and CF-WAC. Each sub-figure consists of a rotor angle of generator 15 (G15), AVR output of G15, the terminal active power output of G15, and active power flow in a line connected between buses 53 and 54. It can be seen that FS-WAC, SP-WAC, and CF-WAC gives the excellent performance in damping out oscillations. As mentioned earlier, in the case of RS-WAC, output signals are given to the generators 13, 14, 15, and 16. But, here, the signal to the generator 15 is lost. Hence, RS-WAC not able to damp out the oscillations. The corresponding settling times are listed in Table 6.

B. LOSS OF TWO COMMUNICATION SIGNALS ON CONTROLLER OUTPUT SIDE

In this case, the performances of the controllers are evaluated by considering the transmitted signals to the generators 13 and 15 lost. The corresponding dynamic waveforms are shown in Fig. 13 and the settling times of all generators are shown in Table 7. From the results, it can be observed that FS-WAC and SP-WAC performances are degraded compared to the previous case. On the other hand, CF-WAC performance does not deteriorate due to communication loss on the controller's output side.

C. LOSS OF ONE COMMUNICATION SIGNAL ON CONTROLLER INPUT SIDE

Fig. 14 represents the dynamic waveforms for the communication loss on the input side of the controller. The loss of

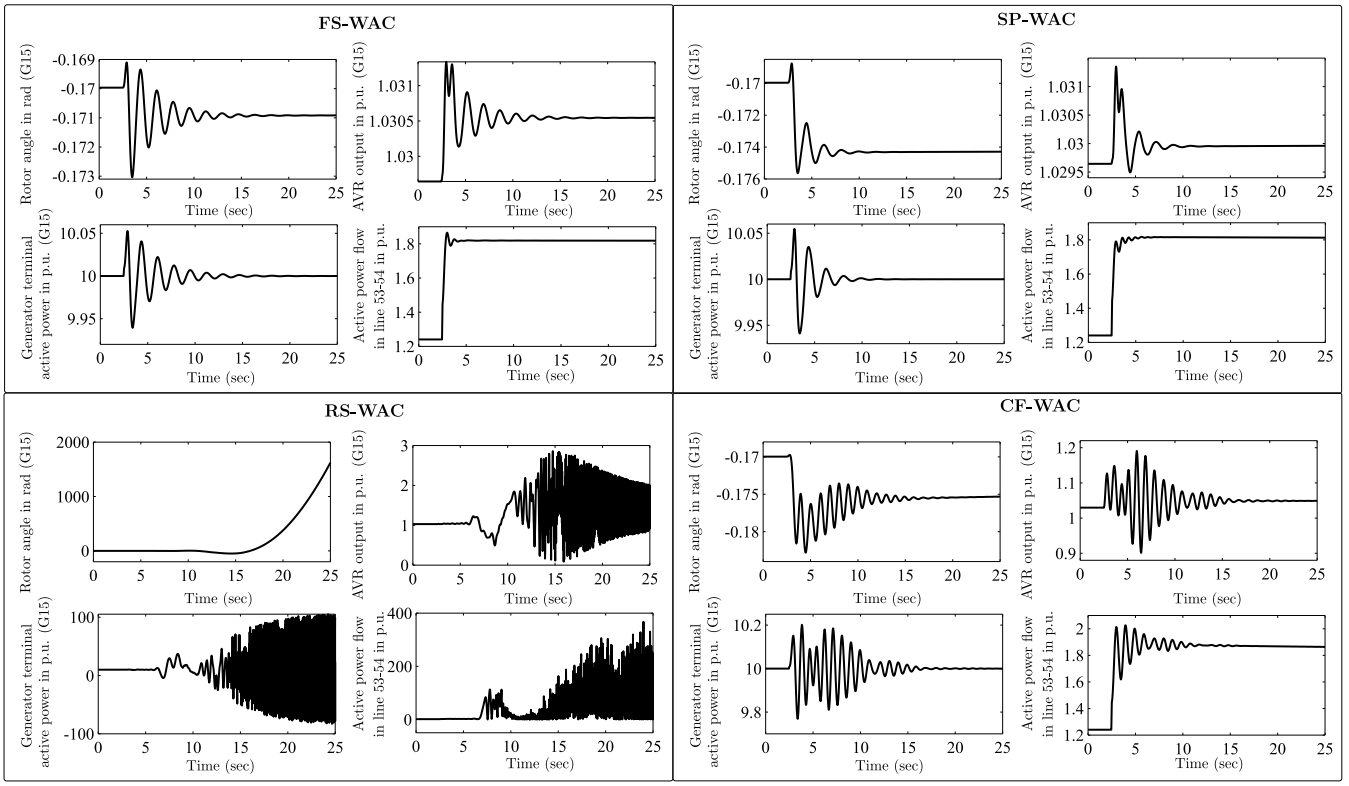

FIGURE 12. The dynamic simulation waveforms for the loss of one communication channel on the controller output side.

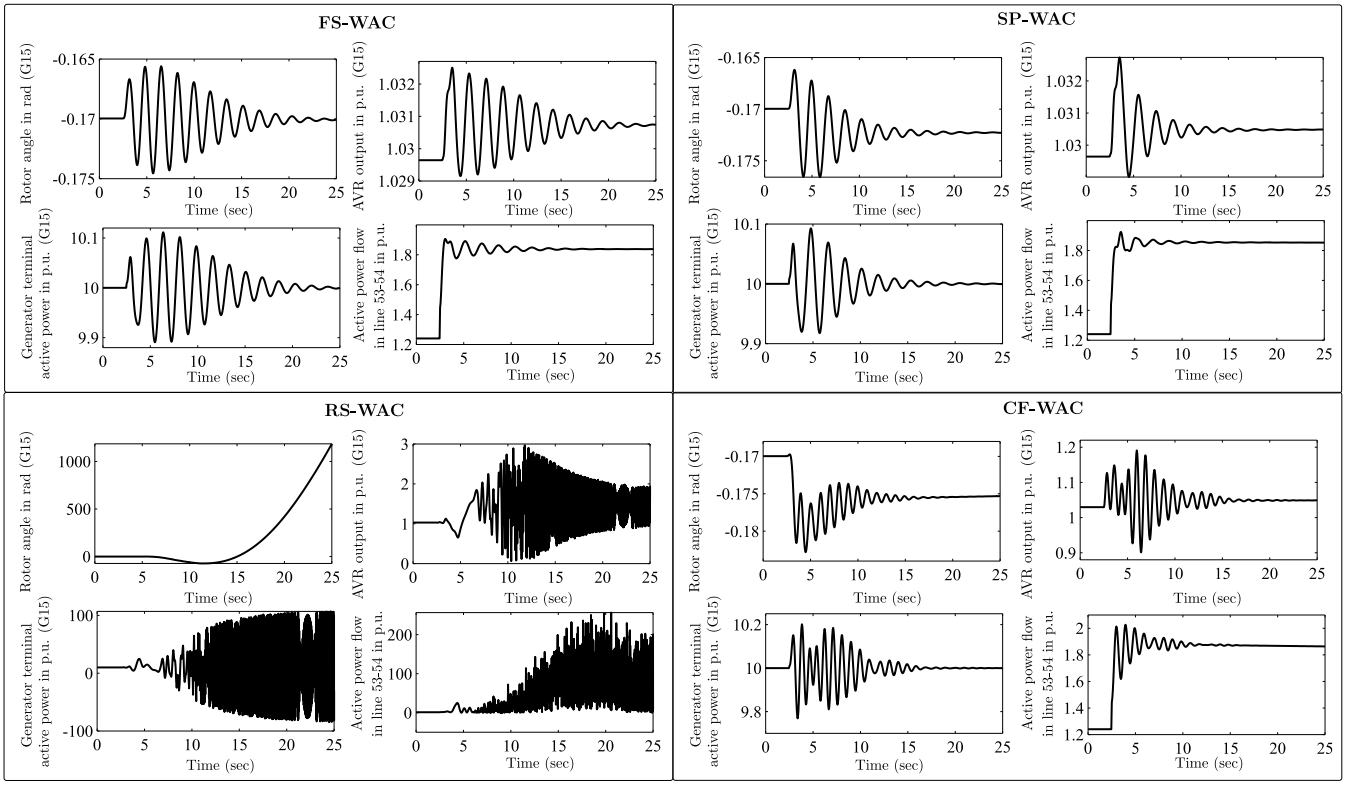

FIGURE 13. The dynamic simulation waveforms for the loss of two communication channels on the controller output side.

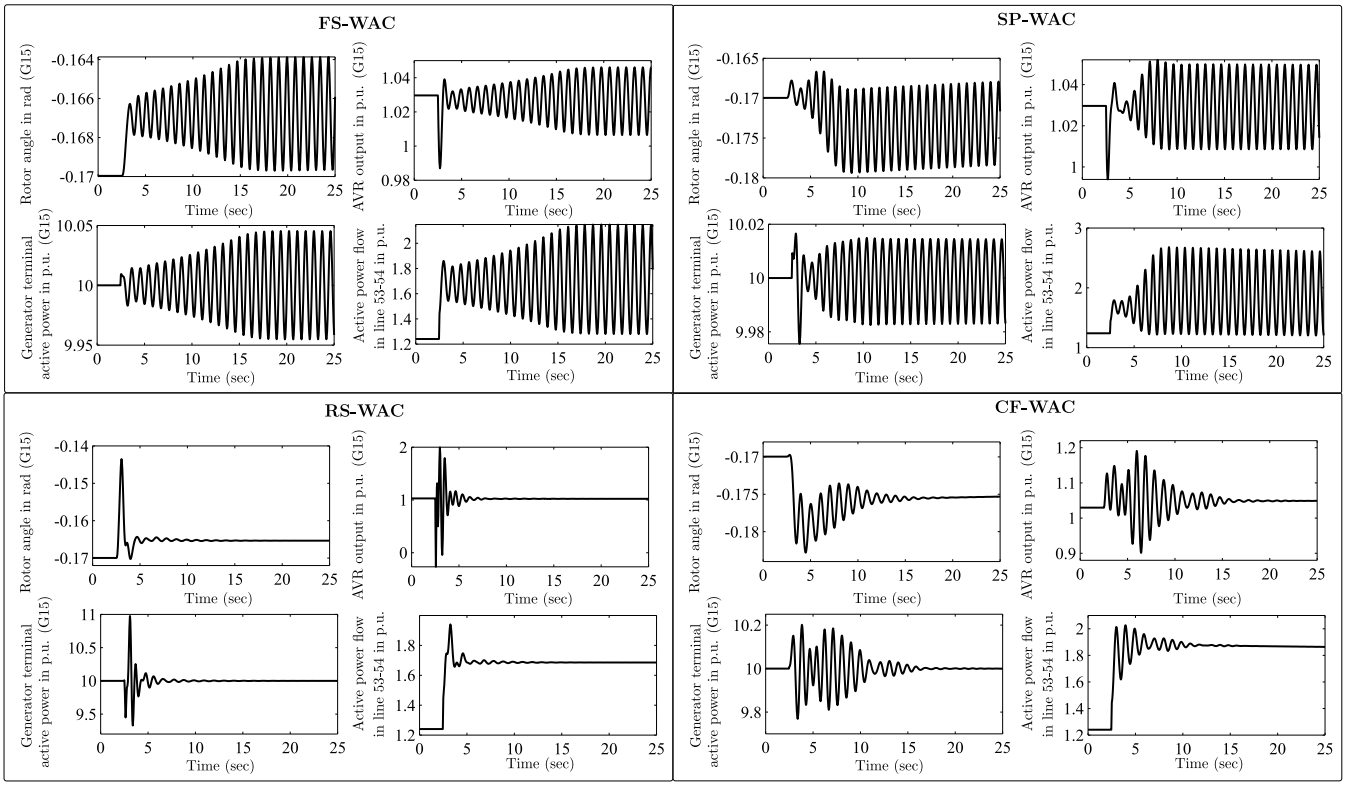

FIGURE 14. The dynamic simulation waveforms for the loss of one communication channel on the controller input side.

TABLE 8. The settling times of all generators considering one communication failure on controller input side.

Gen. Id	FS-WAC	SP-WAC	RS-WAC	CF-WAC
G1	Unstable	Unstable	11.2728	15.2871
G2	Unstable	Unstable	12.0364	18.4921
G3	Unstable	Unstable	12.0037	21.0448
G4	Unstable	Unstable	13.0900	22.0763
G5	Unstable	Unstable	14.6107	23.4381
G6	Unstable	Unstable	13.0900	23.1987
G7	Unstable	Unstable	12.6508	22.1127
G8	Unstable	Unstable	11.2837	21.5982
G9	Unstable	Unstable	15.0283	16.5432
G10	Unstable	Unstable	9.5887	15.5062
G11	Unstable	Unstable	9.6999	20.1000
G12	Unstable	Unstable	9.1190	21.8193
G13	Unstable	Unstable	9.1487	12.5077
G14	Unstable	Unstable	11.8542	17.6271
G15	Unstable	Unstable	7.9544	19.5275
G16	Unstable	Unstable	12.3134	17.1647

generator 7 (G7) signal carried by PMU to the controller input is considered. The corresponding settling times are tabulated in Table 8. From the results, it can be observed that FS-WAC and SP-WAC cannot be able to damp out the oscillations. On the other hand, RS-WAC and CF-WAC are damped out of the oscillations effectively. RS-WAC takes the input signals from generators 13, 14, 15, and 16 only. Therefore, RS-WAC gives excellent performance compared to the remaining controllers.

D. LOSS OF TWO COMMUNICATION SIGNALS ON CONTROLLER INPUT SIDE

In this case, it is assumed that the remote signals of generators 7 (G7) and 15 (G15) transmitted to the controller are lost. The corresponding waveforms are shown in Fig. 15. It can be seen that FS-WAC, SP-WAC and RS-WAC are not able to damp out the oscillations. Since G15 signal is lost, RS-WAC not able to damp out the oscillations. However, CF-WAC alone gives the good performance in damping out the oscillations. The settling times of all generators are listed in 9.

E. LOSS OF ONE COMMUNICATION SIGNAL ON CONTROLLER INPUT SIDE AND ONE SIGNAL ON CONTROLLER OUTPUT SIDE

Here, the loss of generator 7 (G7) signal on controller input side and the loss of transmitted signal to the generator 15 (G15) are considered. Fig. 16 represents the dynamic waveforms of FS-WAC, SP-WAC, RS-WAC and CF-WAC. The settling times are displayed in Table 10. From the results, it is observed that CF-WAC alone gives the good damping performance.

VII. DISCUSSION

The comparison between FS-WAC, SP-WAC, RS-WAC, and CF-WAC is illustrated in this subsection. As mentioned earlier, the proposed CF-WAC does not requires any

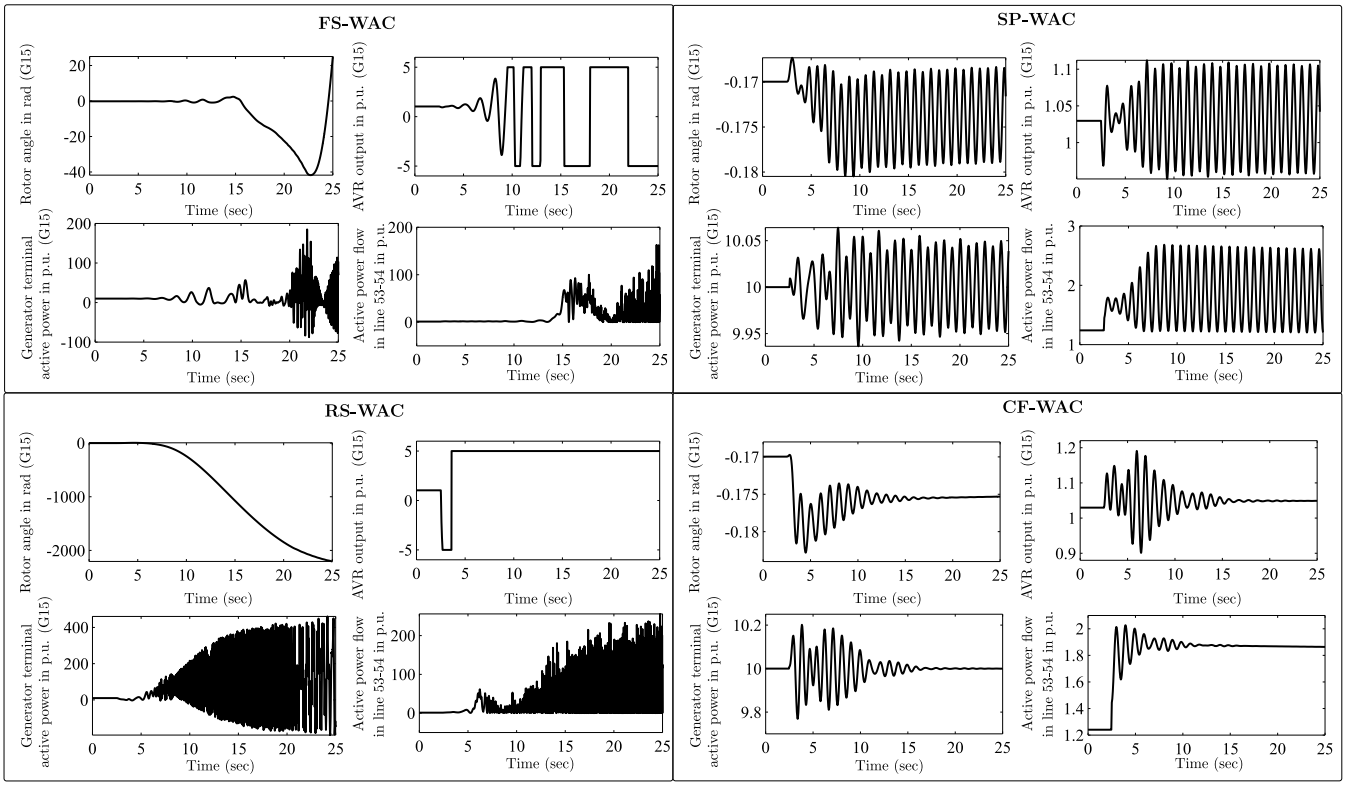

FIGURE 15. The dynamic simulation waveforms for the loss of two communication channels on the controller input side.

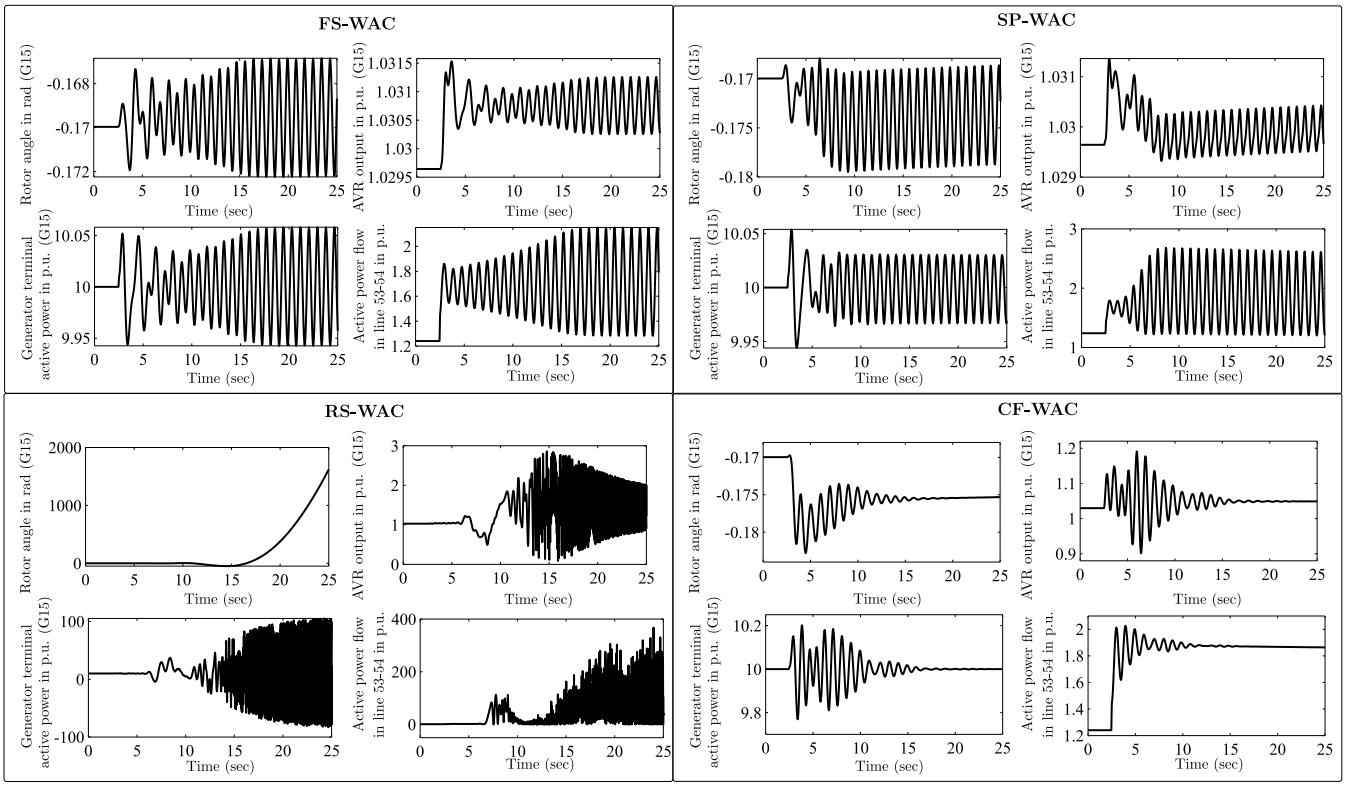

FIGURE 16. The dynamic simulation waveforms for the loss of one communication channel on the controller input and output sides.

TABLE 9. The settling times of all generators considering two communication failures on controller input side.

Gen. Id	FS-WAC	SP-WAC	RS-WAC	CF-WAC
G1	Unstable	Unstable	Unstable	15.2871
G2	Unstable	Unstable	Unstable	18.4921
G3	Unstable	Unstable	Unstable	21.0448
G4	Unstable	Unstable	Unstable	22.0763
G5	Unstable	Unstable	Unstable	23.4381
G6	Unstable	Unstable	Unstable	23.1987
G7	Unstable	Unstable	Unstable	22.1127
G8	Unstable	Unstable	Unstable	21.5982
G9	Unstable	Unstable	Unstable	16.5432
G10	Unstable	Unstable	Unstable	15.5062
G11	Unstable	Unstable	Unstable	20.1000
G12	Unstable	Unstable	Unstable	21.8193
G13	Unstable	Unstable	Unstable	12.5077
G14	Unstable	Unstable	Unstable	17.6271
G15	Unstable	Unstable	Unstable	19.5275
G16	Unstable	Unstable	Unstable	17.1647

TABLE 10. The settling times of all generators considering one communication failure on controller input side and controller output side.

Gen. Id	FS-WAC	SP-WAC	RS-WAC	CF-WAC
G1	Unstable	Unstable	Unstable	15.2871
G2	Unstable	Unstable	Unstable	18.4921
G3	Unstable	Unstable	Unstable	21.0448
G4	Unstable	Unstable	Unstable	22.0763
G5	Unstable	Unstable	Unstable	23.4381
G6	Unstable	Unstable	Unstable	23.1987
G7	Unstable	Unstable	Unstable	22.1127
G8	Unstable	Unstable	Unstable	21.5982
G9	Unstable	Unstable	Unstable	16.5432
G10	Unstable	Unstable	Unstable	15.5062
G11	Unstable	Unstable	Unstable	20.1000
G12	Unstable	Unstable	Unstable	21.8193
G13	Unstable	Unstable	Unstable	12.5077
G14	Unstable	Unstable	Unstable	17.6271
G15	Unstable	Unstable	Unstable	19.5275
G16	Unstable	Unstable	Unstable	17.1647

communication paths on both input and output side of the controller. On the other hand, FS-WAC, SP-WAC, and RS-WAC requires communication paths. Table 11 represents the performances of controllers for different disturbances. From Table 11, it can be observed that FS-WAC and SP-WAC gives the superior performance in the case of line outage, load shedding and three phase fault. In the case of communication signal loss, the proposed CF-WAC alone gives the excellent performance compared to remaining all controllers.

A. PERFORMANCE OF CF-WAC AGAINST LOSS OF SPEED AND ANGLE MEASUREMENTS

In previous sections, the performance of FS-WAC, SP-WAC, RS-WAC, and CF-WAC against the loss of communication channels are illustrated. However, CF-WAC doesn't require any communication paths. Therefore, in this subsection, the performance of CF-WAC against missing of speed and angle measurements is illustrated by considering two cases. In first case, missing of generator 7 (G7) speed and angle

TABLE 11. The performance comparison between FS-WAC, SP-WAC, RS-WAC, and CF-WAC.

Disturbance Id	FS-WAC	SP-WAC	RS-WAC	CF-WAC
TL_OUT	Excellent	Excellent	Good	Good
LD_SHD	Excellent	Excellent	Good	Good
3_PH_FLT	Excellent	Excellent	Good	Good
1_OP_LOSS	Excellent	Excellent	Poor	Good
2_OP_LOSS	Good	Good	Poor	Excellent
1_IP_LOSS	Poor	Poor	Excellent	Excellent
2_IP_LOSS	Poor	Poor	Poor	Excellent
1_IP_1_OP_LOSS	Poor	Poor	Poor	Excellent

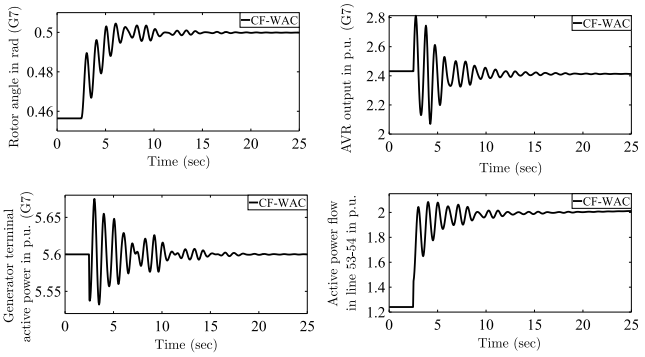

FIGURE 17. The dynamic simulation waveforms in the case of G7 measurements lost.

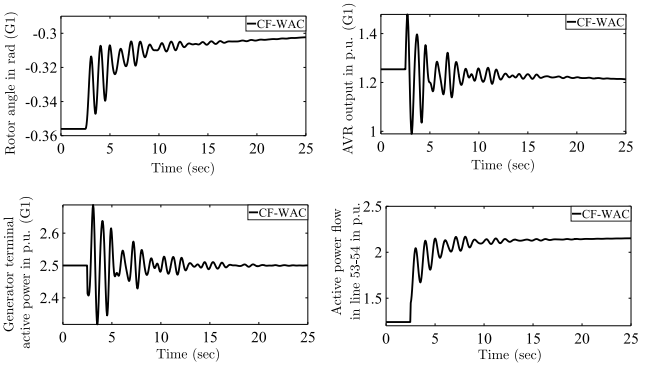

FIGURE 18. The dynamic simulation waveforms in the case of G7 and G15 measurements lost.

measurements is considered. The corresponding dynamic waveforms are shown in Fig. 17. In second case, missing of speed and angle measurements of G7 and G15 are considered. The corresponding dynamic waveforms are shown in Fig. 18. From these results, it can be observed that the proposed WAC (CF-WAC) gives the good damping performance even under the loss of measurements.

B. VALIDATION OF THE PROPOSED CONTROLLER's (CF-WAC) ROBUSTNESS

In this subsection, the robustness and reliability of the proposed controller is verified against changes in power system network structures such as continuous line outages and three line outages at a time. In continuous line outages, three lines are opened at different time intervals. The first

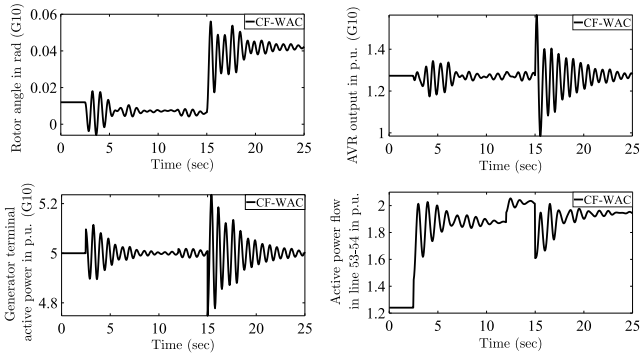

FIGURE 19. The dynamic simulation waveforms for the continuous line outages.

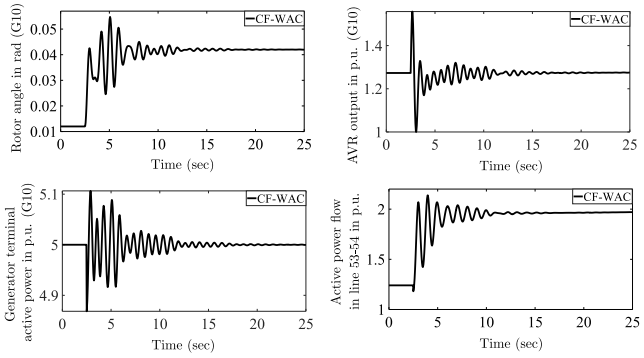

FIGURE 20. The dynamic simulation waveforms for the three line outages at a time.

line connected between buses 60 and 61 is disconnected at 2.5 sec, second line connected between buses 27 and 53 opened at 12 sec, and the last line connected between buses 36 and 61 is opened at 15 sec. The corresponding dynamic waveforms are shown in Fig. 19. Fig. 20 represents the dynamic waveforms for three lines connected between buses 60-61, 27-53, and 36-61 are opened at a time at 2.5 sec. Earlier, the proposed controller's performance is verified against different disturbances as shown in Table 2. Therefore, from these results, it can be seen that the proposed controller is able to provide sufficient damping under different disturbances and power system network changes.

VIII. CONCLUSION

In this paper, fault-tolerant wide-area controller design is proposed to damp out inter-area oscillations, which requires no communication channels. In addition, the performance of the proposed CF-WAC is compared with FS-WAC, SP-WAC, and RS-WAC. The structurally constrained H_2-norm optimization technique is used to design FS-WAC, SP-WAC, RS-WAC, and CF-WAC. The proposed CF-WAC is designed in a centralized manner. However, later, it is separated into different groups that give a decentralized structure corresponding to speed and angle states alone. Thus, no communication lines are required to transmit wide-area controller signals to the excitation system of generators. The effectiveness of CF-WAC is verified by considering different disturbances and loss of communication channels. From the results, it is observed that the proposed CF-WAC is able to damp out low-frequency oscillations within a specific amount of time. On the other hand, FS-WAC and SP-WAC give good performance compared to the proposed CF-WAC. RS-WAC and CF-WAC are offering almost the same performance. However, the performances of FS-WAC, SP-WAC, and RS-WAC are deteriorated when the data is lost due to communication channels. The proposed CF-WAC performance is constant when there is communication loss or not. Therefore, it is quite enough to design the wide-area controller by considering speed and angle states, which requires no communication paths.

REFERENCES

[1] G. Rogers, *Power System Oscillations*. Norwell, MA, USA: Kluwer, 2000.
[2] P. Kundur, *Power System Stability and Control*. New York, NY, USA: McGraw-Hill, 1994.
[3] B. Chaudhuri, R. Majumder, and B. C. Pal, "Wide-area measurement-based stabilizing control of power system considering signal transmission delay," *IEEE Trans. Power Syst.*, vol. 19, no. 4, pp. 1971–1979, Nov. 2004.
[4] Y. Zhang and A. Bose, "Design of wide-area damping controllers for inter-area oscillations," *IEEE Trans. Power Syst.*, vol. 23, no. 3, pp. 1136–1143, Aug. 2008.
[5] C. W. Taylor, D. C. Erickson, K. E. Martin, R. E. Wilson, and V. Venkatasubramanian, "WACS-wide-area stability and voltage control system: R&D and online demonstration," in *Proc. IEEE*, vol. 93, no. 5, pp. 892–906, May 2005.
[6] D. Dotta, A. S. E. Silva, and I. C. Decker, "Wide-area measurements-based two-level control design considering signal transmission delay," *IEEE Trans. Power Syst.*, vol. 24, no. 1, pp. 208–216, Feb. 2009.
[7] A. C. Zolotas, B. Chaudhuri, I. M. Jaimoukha, and P. Korba, "A study on LQG/LTR control for damping inter-area oscillations in power systems," *IEEE Trans. Control Syst. Technol.*, vol. 15, no. 1, pp. 151–160, Jan. 2007.
[8] F. Lin, M. Fardad, and M. R. Jovanović, "Design of optimal sparse feedback gains via the alternating direction method of multipliers," *IEEE Trans. Autom. Control*, vol. 58, no. 9, pp. 2426–2431, Sep. 2013.
[9] F. Dorfler, M. R. Jovanović, M. Chertkov, and F. Bullo, "Sparsity-promoting optimal wide-area control of power networks," *IEEE Trans. Power Syst.*, vol. 29, no. 5, pp. 2281–2291, Sep. 2014.
[10] N. Reddy Naguru and Y. Babu G. V. N., "Reduced-scale wide area control system design based upon the dominancy index analysis," in *Proc. 8th Int. Conf. Power Syst. (ICPS)*, Jaipur, India, Dec. 2019, pp. 1–5.
[11] B. Chaudhuri, B. C. Pal, A. C. Zolotas, I. M. Jaimoukha, and T. C. Green, "Mixed-sensitivity approach to H_∞ control of power system oscillations employing multiple FACTS devices," *IEEE Trans. Power Syst.*, vol. 18, no. 3, pp. 1149–1156, Aug. 2003.
[12] I. Kamwa, R. Grondin, and Y. Hebert, "Wide-area measurement based stabilizing control of large power systems—A decentralized/hierarchical approach," *IEEE Trans. Power Syst.*, vol. 16, no. 1, pp. 136–153, Feb. 2001.
[13] J. H. Chow, J. J. Sanchez-Gasca, H. Ren, and S. Wang, "Power system damping controller design using multiple input signals," *IEEE Control Syst.*, vol. 20, no. 4, pp. 82–90, Aug. 2000.
[14] W. Yao, L. Jiang, J. Wen, Q. H. Wu, and S. Cheng, "Wide-area damping controller of FACTS devices for inter-area oscillations considering communication time delays," *IEEE Trans. Power Syst.*, vol. 29, no. 1, pp. 318–329, Jan. 2014.
[15] S. Zhang and V. Vittal, "Design of wide-area power system damping controllers resilient to communication failures," *IEEE Trans. Power Syst.*, vol. 28, no. 4, pp. 4292–4300, Nov. 2013.

[16] N. R. Chaudhuri, B. Chaudhuri, S. Ray, and R. Majumder, "Wide-area phasor power oscillation damping controller: A new approach to handling time-varying signal latency," *IET Generat., Transmiss. Distrib.*, vol. 4, no. 5, pp. 620–630, May 2010.
[17] B. P. Padhy, S. C. Srivastava, and N. K. Verma, "A wide-area damping controller considering network input and output delays and packet drop," *IEEE Trans. Power Syst.*, vol. 32, no. 1, pp. 166–176, Jan. 2017.
[18] M. E. C. Bento, D. Dotta, R. Kuiava, and R. A. Ramos, "A procedure to design fault-tolerant wide-area damping controllers," *IEEE Access*, vol. 6, pp. 23383–23405, 2018.
[19] F. R. Segundo Sevilla, I. Jaimoukha, B. Chaudhuri, and P. Korba, "Fault-tolerant control design to enhance damping of inter-area oscillations in power grids," *Int. J. Robust Nonlinear Control*, vol. 24, nos. 8–9, pp. 1304–1316, May 2014.
[20] Y. Shen, W. Yao, J. Wen, H. He, and L. Jiang, "Resilient wide-area damping control using GrHDP to tolerate communication failures," *IEEE Trans. Smart Grid*, vol. 10, no. 3, pp. 2547–2557, May 2019.
[21] A. K. Jain and V. T. Ranganathan, "Modeling and field oriented control of salient pole wound field synchronous machine in stator flux coordinates," *IEEE Trans. Ind. Electron.*, vol. 58, no. 3, pp. 960–970, Mar. 2011.
[22] E. Ghahremani and I. Kamwa, "Dynamic state estimation in power system by applying the extended Kalman filter with unknown inputs to phasor measurements," *IEEE Trans. Power Syst.*, vol. 26, no. 4, pp. 2556–2566, Nov. 2011.
[23] E. Ghahremani and I. Kamwa, "Online state estimation of a synchronous generator using unscented Kalman filter from phasor measurements units," *IEEE Trans. Energy Convers.*, vol. 26, no. 4, pp. 1099–1108, Dec. 2011.
[24] N. R. Naguru, "Towards an enhanced wide area control system for damping out low frequency oscillations in power grid," Ph.D. dissertation, Indian Inst. Technol. Hyderabad, Hyderabad, India, 2019.

NAGASEKHARA REDDY NAGURU (Member, IEEE) received the M.Tech. degree in power systems from the National Institute of Technology (NIT) Tiruchirappalli, India, in 2011, and the Ph.D. degree from IIT Hyderabad, India, in 2019. He is currently working as an Associate Professor with the Department of Electrical and Electronics Engineering, Stanley College of Engineering and Technology for Women, Hyderabad, India. His research interests include wide-area monitoring and control, power system stability analysis and control, smart grid, and renewable energy integration.

YATENDRA BABU GANAPAVARAPU (Member, IEEE) received the M.Tech. degree in power electronics and power systems from IIT Hyderabad, India, in 2013. He submitted his Ph.D. thesis at the Department of Electrical Engineering, IIT Hyderabad. His research interests include power system stability, flexible grids, power system visualization, and transactive energy systems.